Reproductive Sciences (2024) 31:2718–2730
https://doi.org/10.1007/s43032-024-01526-7

ENDOMETRIUM: ORIGINAL ARTICLE

The Essential Role of PGF2α/PTGFR in Molding Endometrial Breakdown and Vascular Dynamics, Regulated by HIF-1α in a Mouse Menstrual-like Model

Fang Zhou[1,2] · Shufang Wang[4] · Wenhong Lu[2] · Xihua Chen[3] · Shige Guo[1,3] · Cong Lu[1,3] · Xin Zhang[1,3] · Jiangxu Wu[1,3] · Siyu Wang[1,3] · Zeyi Long[1,3] · Bin He[3] · Taifeng Zhuang[5] · Xiangbo Xu[3]

Received: 3 January 2024 / Accepted: 19 March 2024 / Published online: 18 April 2024

Abstract

In women of childbearing age, extensive decidualization, shedding and remodeling of the endometrium during the menstrual cycle are fundamental for successful pregnancy. The role of prostaglandins (PGs) in menstruation has long been proposed in humans, and the rate-limiting enzyme cyclooxygenase was shown to play a key role in endometrial breakdown and shedding in a mouse menstrual-like model in our previous study. However, the specific types of PGs involved and their respective roles remain unclear. Therefore, our objective was to investigate the mechanism through which PGs regulate endometrial disintegration. In this study, the microscopy was observed by HE; the protein levels of prostaglandins E1 (PGE1), prostaglandins E2 (PGE2), prostaglandin F2α (PGF2α) and Prostaglandin I2 (PGI2) were detected by ELISA; the mRNA level of *Pfgfr2*, Vascular Endothelial Growth Factor(*Vegf*), *Angiostatin* and Hypoxia inducible factor-1α (*Hif1α*) were examined by real-time PCR; PTGFR Receptor (PTGFR), VEGF, Angiostatin and HIF-1α protein levels were investigated by western blotting; the locations of protein were observed by Immunohistochemistry; HIF-1α binding PTGFR promoter was detected by Chromatin Immunoprecipitation (ChIP) and real-time PCR. We found that the concentrations of PGE1, PGE2, and PGF2α all increased significantly during this process. Furthermore, *Ptgfr* mRNA increased soon after Progesterone (P4) withdrawal, and PTGFR protein levels increased significantly during abundant endometrial breakdown and shedding processes. PTGFR inhibitors AL8810 significantly suppressed endometrial breakdown and shedding, promoted Angiostatin expression, and reduced VEGF-A expressions and vascular permeability. And HIF-1α and PTGFR were mainly located in the luminal/gland epithelium, vascular endothelium, and pre-decidual zone. Interestingly, HIF-1α directly bound to *Ptgfr* promoter. Moreover, a HIF-1α inhibitor 2-methoxyestradiol (2ME) significantly reduced PTGFR expression and suppressed endometrial breakdown which was in accord with PTGFR inhibitor's effect. Similar changes occurred in human stromal cells relevant to menstruation in vitro. Our study provides evidence that PGF2α/PTGFR plays a vital role in endometrial breakdown via vascular changes that are regulated by HIF-1α during menstruation.

Keywords Prostaglandins F · Prostaglandin receptor · Hypoxia-inducible factor 1 · Capillary permeability · Menstruation

✉ Xiangbo Xu
xiangboxuhappy@126.com

[1] Chinese Academy of Medical Sciences & Peking Union Medical College, Beijing, China

[2] Human Sperm Bank, National Research Institute for Family Planning, Beijing, China

[3] Reproductive Physiology Laboratory, NHC Key Laboratory of Reproductive Health Engineering Technology Research, National Research Institute for Family Planning, Beijing, China

[4] Department of Forensic Medicine, Xinxiang Medical University, Xinxiang, Henan Province, China

[5] Beijing Obstetrics & Gynecology Hospital, Capital Medical University, Beijing Maternal &. Child Health Care Hospital, Beijing, China

Introduction

In women of childbearing age, the functional layer of the endometrium undergoes extensive breakdown and remodeling under the influence of hormonal regulation during the menstrual cycle, which is fundamental for successful pregnancy. In 1957, it was reported that menstrual fluid contained substances with characteristics of prostaglandins (PGs), which were later identified as Prostaglandin F2α (PGF2α) and Prostaglandin E2 (PGE2) [1]. Interestingly, the levels of these substances in the menstrual fluid show cyclic changes, especially in the secretory phase and during menstruation. PGs, which are members of a group of hormonally active fatty acids, are short-range lipid signaling molecules. PGs signaling begins with arachidonic acid converted into prostaglandin intermediates prostaglandin G2 (PGG2) and prostaglandin H2 (PGH2) by the rate-limiting enzyme Cyclooxygenase (COX) [2]. All other PGs [Prostaglandin I2 (PGI2), PGE2, PGF2α, Prostaglandin D2 (PGD2), and Thromboxane 2 (TXA2)] are derived from PGH2 via a variety of prostanoid synthases and isomerases [3]. Furthermore, prostanoids function through G-protein coupled receptors.

PGs have the effect of enhancing uterine contraction and play a major role in menstrual bleeding [4]. It has been hypothesized that PGs might cause spiral arterioles constriction in the endometrium, ultimately leading to endometrial breakdown and menstruation [5]. In our previous study, we explored COX regulates endometrial breakdown using a mouse menstrual-like model, which provide evidence that PGs play an important role in triggering menstruation [6]. However, which PGs signaling molecules play a dominant role in endometrial disintegration in mouse menstrual-like model remains to be further explored.

PGF2α, acting through its receptor PGF2α Receptor (PTGFR), is a vasoconstrictor and might induce uterine myometrium contractility and can also increase the permeability of the bronchial artery [7]. In a previous study, PGF2α induced Vascular endothelial growth factor (VEGF) expression in female reproduction, such as luteolysis, implantation, and cell proliferation in the endometrium [8]. VEGF is a key factor in angiogenesis that regulates vascular permeability and neutrophil influx into the uterus. Moreover, angiostatin, a proteolytic fragment of plasminogen, is a potent endogenous anti-angiogenic agent that can induce vascular regression in tumors and inhibit the activation and migration of neutrophils [9, 10]. Therefore, we hypothesized that PGF2α/PTGFR regulates VEGF and angiostatin, affecting vascular permeability during endometrial breakdown.

In humans, it was assumed that tissue hypoxia may cause endometrial breakdown due to vasoconstriction of spiral arterioles [11]. However, in our previous study, we found that hypoxia was involved but was not essential for endometrial breakdown, and hypoxia-inducible factor 1-alpha (HIF-1α) is activatedduring endometrial breakdown in a mouse menstrual-like model and has been identified in the human endometrium during the menstrual phase [12–14]. In previous study, it had been demonstrated that hypoxia acts via HIF-1α to increase VEGF, whereas PGF2α induces VEGF expression independently of HIF-1α during human endometrial repair [15]. The relationship between HIF-1α and PGF2α/PTGFR during endometrial breakdown is unclear.

In this study, based on the mouse menstrual-like model, we investigated the dynamic changes in PGE1, PGE2, and PGF2α levels during endometrial breakdown in a mouse menstrual-like model. Furthermore, we elucidated that PGF2α/PTGFR, played a key role in this process via changes in vascular permeability, which were regulated by HIF-1α in the mouse menstrual-like model.

Materials and Methods

Mouse Menstrual-Like Model System

All experimental and surgical procedures were approved by the Animal Ethics Committee of the National Research Institute for Family Planning. 8 weeks old virgin C57BL/6 J mice (19–20 g) were obtained from the Institute of Laboratory Animal Services, Chinese Academy of Medical Sciences. The mice were maintained under controlled conditions with unrestricted access to food and water.

Animal manipulations were performed following the procedures as previously described [16]. Briefly, mice were ovariectomized and recovered for two weeks. Then, on days 1–3, the mice were subcutaneously (s.c.) injected with 100 ng of 17β-estradiol (17-E2; Alfa Aesar Inc., United Kingdom). On day 7, 5 ng of 17-E2 and 50 ng of Progesterone (P4) (Sigma Aldrich, USA) were injected s.c. and P4 implants were inserted into the back of each mouse. On days 8–9, 5 ng of 17-E2 was injected s.c.. On day 9, 15 µL arachis oil was injected into the lumen of the uterine horns to induce decidualization. Control groups were injected 0.9% saline solution 0.49 h after, the P4 implants were removed (P4 withdrawal, regarded as 0 h). Mice from both the treatment and control groups were sacrificed at 0, 8, 12, 16, and 24 h after P4 withdrawal (total $n = 15–20$ mice/time point). Their uterine horns were collected and stored in 4% paraformaldehyde solution or at -80 °C for further analysis. The uterine specimens underwent pathological processing, being embedded in paraffin and subsequently sectioned. Histological observation was carried out through Hematoxylin and Eosin (HE) staining.

Mice in the menstrual-like model were treated with intraperitoneal (i.p.) injections of the PTGFR inhibitor AL8810 (APExBIO b4575; 10 mg/kg) dissolved in PBS with 2% DMSO, as well as the HIF-1α inhibitor 2-methoxyestradiol (2ME, Selleck, S1233, 100 mg/kg) dissolved in arachis oil with 2% DMSO, at 4 h before P4 withdrawal, and at 4 h and 12 h after P4 withdrawal ($n=3$ for each time point). The corresponding solvent were served as negative controls. The percentage of endometrial breakdown was represented by the ratio of endometrial breakdown zone to total decidual zone [17].

Each mouse was injected with 100 μL of 2% Evans blue physiological saline solution by tail vein injection. The mice were euthanized 30 min later. The entire uterine tissue was weighed and placed in a test tube containing 450 μL formamide solution for 24 h ($n=3$). The relative content of Evans blue in a formamide solution was detected using a 620 nm wavelength spectrophotometer. The vascular permeability was directly proportional to the Evans blue content per uterine tissue weight.

Enzyme-Linked Immunosorbent Assay (ELISA)

PGF2, PGE1, PGE2, and PGI2 concentrations in mouse uteri were determined using the following ELISA kits: Prostaglandin F2 ELISA Kit, Cayman, No. 516011; Prostaglandin E1 ELISA Kit, Enzo, No. ADI-900–005; Prostaglandin E2 ELISA kit, R&D SYSTEMS, KGE004B; Urinary Prostacyclin (PGI2) ELISA Kit, Enzo, No. ADI-900–025. Approximately 20 mg of each uteri samples was homogenate and extracted to a consistent dilution rate, and then performed according to the manufacturer's instructions.

Real-Time PCR

Total RNA extraction and real-time PCR were performed according to the manufacturer's instructions. Firstly, RNA was extracted using TRIzol reagent (Invitrogen, USA) ($n=3$). First Strand cDNA Synthesis Kit (PrimeScript RT Master Mix, RR036A, TAKARA) was used for cDNA synthesis. Real-time PCR was performed on a Smart Cycler II System (Applied Biosystems, USA) using SYBR Premix Ex Taq II (TAKARA). The thermal cycling for cDNA amplifications was: initial activation cycle at 95 °C for 10 min, followed by 40 cycles of denaturation (95 °C for 5 s), annealing, and amplification (60 °C for 60 s). The *Ptgfr* primer sequences were as follows: forward, 5'-CATGTTTGCTGTGTTCGTGG-3', reverse, 5'-GTCTTCCCAGTCTTCFATFTG-3'; mouse *Ptger2* forward, 5'-ACCATCTCACCCGCCATATG-3', reverse, 5'-GAGGTCCCACTTTTCCTTTAGG-3'; mouse *β-Actin* forward, 5'-ACCGTGAAAAGATGACCCAG-3', reverse, 5'-GTACGACCAGAGGCATACAG-3'; Mouse *Hif-1α* forward, 5'-TGACTGTGCACCTACTATGTCACTT-3', reverse, 5'-GGTCAGCTGTGGTAATCCACTC-3'. All values were normalized to the *β-Actin* expression levels. Relative quantification was performed using the $2^{-\Delta\Delta Ct}$ method.

Western Blotting

Cytoplasmic and nuclear extracts of mouse uterine were prepared according to the manufacturer's instructions using the NE-PER Nuclear and Cytoplasmic Extraction Reagents kit (Thermo Scientific, USA), a phosphatase inhibitor (Roche, Germany), and a protease inhibitor (Merck KGaA, Germany). The protein concentrations were determined using colorimetric BCA protein assays (Thermo Scientific, USA), and equal amounts of nuclear and cytoplasmic proteins were subjected to SDS-PAGE Tris–glycine gels (Amresco, USA) and then transferred onto polyvinylidene fluoride membranes (Millipore, Massachusetts). Subsequently, the membranes were blocked for 1 h at room temperature using Tris-buffered saline with Tween 20 (50 mM Tris–HCl, 150 mM NaCl, and 0.1%[v/v] Tween 20) containing 5% (w/v) non-fat dried milk, and were incubated with primary antibodies of PTGFR (1:2500; Abcam, ab176493), PTGER2 (1:2500; Abcam ab124419), Angiostatin (1:1500;Abcam ab154560), VEGFA (Santa Cruz sc-7269), HIF-1α (1:500, NB100-134; Novus Biologicals, USA), LAMIN-B1 (D9V6H) (1:1 000, Cell Signaling Technology, 13435S), or β-ACTIN (1:2000; CoWin, Beijing, China) respectively, overnight at 4 °C. After washing and incubation with the respective secondary antibodies, either anti-goat antibody (1:5000, Zhongshan, Beijing, China) or anti-rabbit antibody (1:10000, Zhongshan, Beijing, China), at room temperature for 1 h, protein bands were detected using an enhanced chemiluminescence system (TransGen, Beijing, China) and quantified using Quantity One software (Bio-Rad, California).

Immunohistochemical Analysis

Briefly, the serial cross-sections were rehydration, and then treated with an antigen retrieval procedure (citrate buffer, pH 6.0; 98 °C for 20 min). Sections were incubated in 3% H_2O_2 at room temperature for 10 min to quench endogenous hydrogen peroxidase activity. Non-specific staining was blocked with 5% goat serum for 30 min at room temperature. Sections were then incubated with rabbit anti-PTGFR antibody (1:200, ab203342, Abcam), rabbit anti-PTGER2 antibody (1:200, ab124419, Abcam) or rabbit anti-HIF-1α (1:100, NB100-479; Novus Biologicals) overnight at 4 °C. Matched rabbit non-immune immunoglobulin G (IgG) was used as the negative control. Subsequently, the sections were treated with secondary antibodies (PV-6001 or PV-6002; Zhongshan, China) for 30 min at 37 °C. The protein immunoactivity was visualized using

a 3,3-diaminobenzidine tetrahydrochloride kit (ZLI-9032, Zhongshan, China), and counterstained with hematoxylin. The sections were dehydrated and finally mounted using neutral balsam mounting medium.

Chromatin Immunoprecipitation Assay (ChIP)

Chromatin immunoprecipitation (ChIP) assay was performed using SimpleChIP® Plus Enzymatic Chromatin IP Kit (9004, Cell Signaling Technology, USA). The assay was performed in accordance with the manufacturer's instructions. Uterine tissues (25 mg/IP) of 3 individual mouse of 0 h and 16 h each were prepared. 10 µl HIF-1A (NB100-134, Novus) were used for each IP. Primers used to detect the *Ptgfr* promoter were as follows: 5'-GCCTTGGTTTTCCTTGTTTCTG-3' and 5'-CTTTTAGCCACCAGGCAACTAC-3'. The result was analyzed using the percent of input method in the following equation: $2^{(\text{CT of the 2\%Input Sample}-\text{CT of the IP Sample})} \times 2\% = \text{Percent total input}$ [18].

Human Endometrial Stromal Cells Culture

The immortalized human endometrial stromal cells (T-HESCs) initial source was American Type Culture Collection (ATCC) (CRL-4003). T-HESCs were prepared and cultured as previously described [19]. Decidualization was induced by incubating the stromal cells in a medium containing 2% charcoal-stripped fetal bovine serum, antibiotics (100 U/mL penicillin, 100 mg/mL streptomycin, Gibco), 100 nM medroxy progesterone acetate (MPA; Sigma-Aldrich, USA), 10 nM 17β-E2, and 0.5 mM 8-bromoadenosine 3',5'-cyclic monophosphate sodium salt (cAMP; Sigma-Aldrich) for 8 days. The concentration of prolactin (PRL) in the culture supernatant of the decidual cells was elucidated by a chemiluminescence immunoassay (CLIA). After decidualization, the T-HESCs underwent HIF-1α knock down assay using Lipofectamine™ 3000 (Invitrogen) in accordance with the manufacturer's instructions. Transfection induced *HIF-1α* knockdown in T-HESC cells with *HIF-1α* siRNAs (sense: 5'-CUG AUGACCAGCAACUUGAdTdT-3', antisense sense: 5'-UCA AGUUGCUGUCAUCAGdTdT-3') or scrambled oligonucleotide designed by Shanghai Jima Pharmaceutical Technology. The scrambled oligonucleotide served as negative control. After the transfection treatment lasted for 24 h. After knockdown of *HIF-1α*, the medium was replaced with fresh medium without MPA and 17β-E2, noted as 0 h of P4 withdrawal, and the T-HESCs were harvested at 0, 8, 16, and 24 h. Each experiment was performed independently 3 times. The knockdown of *HIF-1α* were confirmed by *HIF-1α* Real-time PCR applying the following primers: forward 5'-TGGCAGCAA CGACACAGAAACT-3', reverse 5'-TTGGCGTTTCAGCGG TGGGT-3'. Then the relative expression of *PTGFR* mRNA were further investigated by the primers: forward 5'-GAA ATCATTCTCTGGAAACCTGTG-3', reverse 5'-GCATTG ACTGGCAAGCTTATAG-3'. The human β-actinserved as internal control: forward 5'-ACATCCGCAAAGACCTGT AC-3', reverse 5'- TGATCTTCATTGTGCTGGGTG-3'.

Statistical Analysis

The results are expressed as mean values ± SD. The mean values of multiple samples were compared by one-way ANOVA, and mean values of two samples were compared by t-tests. $P < 0.05$ was considered to indicate a significant difference, and $P < 0.01$ was considered a highly significant difference.

Results

PGs Levels in the Uterus during Endometrial Breakdown and Shedding in a Mouse Menstrual-Like Model

PGs include PGF2α, PGE1, PGE2, and PGI. We first studied the PGs levels from 0 to 24 h after P4 withdrawal, which led to endometrial breakdown and shedding (Fig. 1A). Macroscopic observations revealed a light pink in the uterus at 0 h, witch progressively deepens over time, culminating in dark red at 24 h. HE staining of the uterus demonstrated histomorphological features consistent with decidualization at 0 h, and comparable histomorphology persisted until 8 h after P4 withdrawal. At 16 h after P4 withdrawal, most of the decidualized stromal cells were dead. At 24 h after P4 withdrawal, the death of primary decidualized stromal cells were widespread, and the functional layer was shed from the basal layer in the mouse menstrual-like model. The period from 16 to 24 h after P4 withdrawal was the key period for endometrial breakdown and shedding. PGs levels were assessed during this period employing ELISA. Compared to its level at 0 h, PGE1 level was increased significantly at 8 h, 16 h and 24 h after P4 withdrawal compared with 0 h ($P = 0.0065$, $P = 0.0076$ and $P = 0.0470$ respectively) (Fig. 1B). The concentration of PGE2 was low at 0 h and 8 h and then increased at 16 h ($P = 0.0009$), and 24 h ($P = 0.0098$) after P4 withdrawal (Fig. 1C). Moreover, compared to the level at 0 h, PGF2α level increased at 8, 16, and 24 h after P4 withdrawal ($P < 10^{-4}$, $P < 10^{-4}$ and $P = 0.0040$ respectively) (Fig. 1D). However, there was no change in PGI from 0 to 24 h after P4 withdrawal (Fig. 1E), that is, throughout the entire process of endometrial breakdown and shedding. In sum, the protein levels of PGE1, PGE2, and PGF2α increases during endometrial breakdown and shedding in the mouse menstrual-like model.

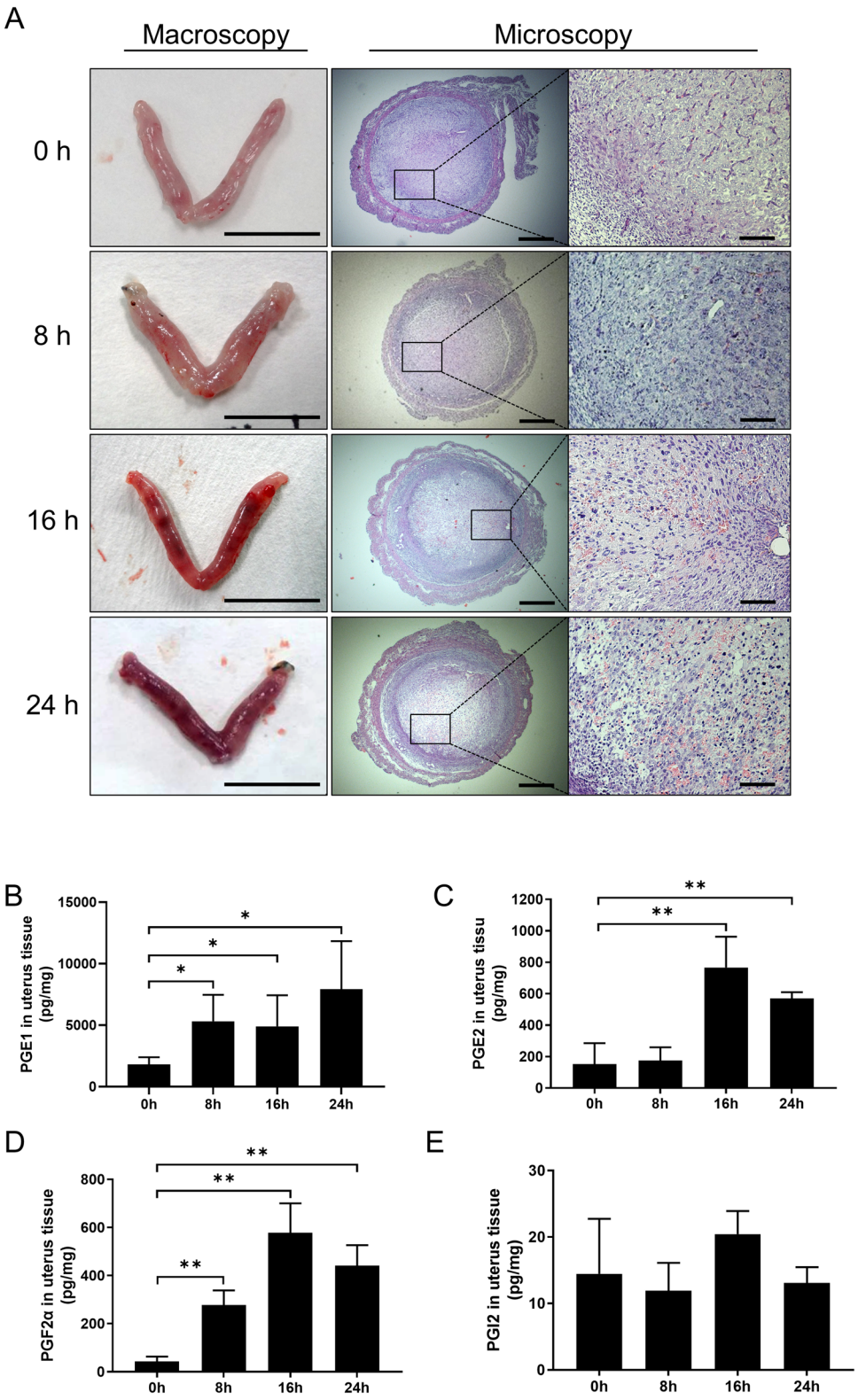

Fig. 1 Macroscopic and morphologic changes and PGs expressions in a mouse menstrual-like model at 0 h, 8 h, 16 h and 24 h after P4 withdrawal **A**: Representative macroscopic and morphological changes in mice menstrual-like model. (The left panel scale bar = 400um; the right panel scale bar = 100 μm.) **B-E**: ELISA detections of PGE1(B), PGE2(C), PGF2α(D) and PGI2(E) protein levels in mice menstrual-like model. (*$P < 0.05$, **$P < 0.01$, $n = 3$)

PTGFR and PTGER2 Expressions in the Uterus during Endometrial Breakdown and Shedding in a Mouse Menstrual-like Model

The expression levels of *Ptger2* and *Ptgfr* mRNA and PTGER2 and PTGFR proteins in the mouse uterus were assayed during whole endometrial breakdown and shedding applying real-time quantitative PCR and western blot assay. *Ptger2* mRNA levels were low at 0–16 h after P4 withdrawal, and increased significantly by 24 h after P4 withdrawal ($P = 0.0065$) (Fig. 2A). However, *Ptgfr* mRNA level increased from 8–24 h after P4 withdrawal relative to 0 h ($P = 0.0002$, $P < 10^{-4}$ and $P = 0.0058$ respectively), and reached a peak at 16 h (Fig. 2B). The levels of PTGER2 significantly reduced from 8 to 24 h, especially at 16 h and 24 h while the endometrium breakdown was abundant ($P = 0.004$ and $P < 10^{-4}$ respectively) (Fig. 2C, D). Moreover, PTGFR protein also showed significantly higher levels from 16–24 h after P4 withdrawal than that at 0–12 h ($P = 0.007$ and $P = 0.003$ respectively) (Fig. 2C, E). Moreover, the locations of PTGFR (Fig. 2F) and PTGER2 (Fig. 2G) proteins in the mouse uterus were also assayed throughout the process of endometrial breakdown and shedding. In the immunoassay, PTGER2 protein was weakly identified in the vascular endothelium, intrauterine epithelium, and decidual stromal cells in the endometrium at 0 h (Fig. 2F). At 8 h after P4 withdrawal, immunostaining results were stronger than those at 0 h, while the locations were similar. At 16 and 24 h, PTGER2 immunostaining resulted in very strong stains, with this protein being located in the intrauterine epithelium, glandular epithelium, and the whole dead decidualized zone. Meanwhile, PTGFR was weakly identified in the primary decidualized zone and strongly identified in the pre-primary decidualized zone at 0 h (Fig. 2G). At 8 h after P4 withdrawal, PTGFR was strongly identified in the intrauterine epithelium and whole decidual cells. At 16 h after P4 withdrawal, the location of the protein was similar to that at 8 h; however, the stains in the pre-primary decidualized zone were stronger than those in the basal layer, where the endometrium was shed.

Role of PTGFR in Endometrial Breakdown and Shedding

To verify the role of PTGFR in endometrial breakdown and shedding, a PTGFR inhibitor AL8810 was administered to the mice before P4 withdrawal. The effect of PTGFR on tissue breakdown was evaluated via gross changes in the uterine horns and endometrial histology from 0–24 h after P4 withdrawal. In the control group, the horns were congested and enlarged, and the color changed from pink to dark red from 0–24 h, indicating uterus bled (Fig. 3A). Histological analysis by HE staining showed that the endometrium decidualized well at 0 h, and there was only a minor degree of necrosis observed under the luminal epithelium at 8 h. The number of necrotic stromal cells in the decidualized zone increased further by 16 h, and nearly all the stromal cells were dead and the whole functional layer was shed from the basal zone till 24 h. Therefore, the endometrium in the control group underwent changes between the processes of decidualization and shedding.

In the group treated with the PTGFR inhibitor AL8810, from 0 to 24 h, the horns were also congested and enlarged, but were always light pink in color throughout the process, indicating that relatively less or no uterine bleeding occurred in the PTGFR inhibitor treatment group (Fig. 3B). The endometrial stromal cells were decidualized at 0 h. At 8–16 h after P4 withdrawal, nearly all the stromal cells in the endometrium had been decidualized and were in a good decidualized state, and there were only a few dead stromal cells under the luminal epithelium. At 24 h after P4 withdrawal, the decidualized zone remained mostly intact, with dead stromal cells observed only at the adjacent area under the luminal epithelium. Moreover, the percentage of endometrial breakdown in the PTGFR inhibitor treatment group was 36.8% at 24 h (Fig. 3C), which was significantly lower than that in the control group ($P = 0.0002$). These results shown that the PTGFR inhibitor could inhibit endometrial breakdown and shedding.

PTGFR Inhibitors Promote Angiostatin Expression and Reduce VEGF Expression and Vascular Permeability

The expression of VEGF and Angiostatin that related to vascular permeability was assessed in the mouse menstrual-like model in control group and PTGFR inhibitor AL8810 group. In the control group, real-time quantitative PCR reveals that *Vegfa* mRNA levels were highest at 16 h after P4 withdrawal, and AL8810 treatment significantly reduced in comparison to those of the control group at 16 h ($P = 0.0024$, $P = 0.0022$ and $P = 0.013$ respectively) (Fig. 4A). A similar pattern was observed for the amount of VEGF protein, investigated through the western blot assay, which was relatively high at 8 h to 24 h after P4 withdrawal (Fig. 4B), and the PTGFR inhibitor also significantly reduced VEGFA protein levels in comparison to the control group at 16 h after P4 withdrawal ($P = 0.0096$). Moreover, *Angiostatin* mRNA in the control group was at a low level from 8–24 h, and the PTGFR inhibitor significantly increased *Angiostatin* mRNA levels at 8–24 h compared to the control group ($P = 0.0038$, $P = 0.0025$ and $P = 0.0162$ respectively) (Fig. 4C), and Angiostatin protein levels were also increased significantly at 16 h ($P = 0.0247$) and 24 h ($P < 10^{-4}$) compared with the control group (Fig. 4D). VEGF and Angiostatin are both related to vascular permeability. The Evans blue

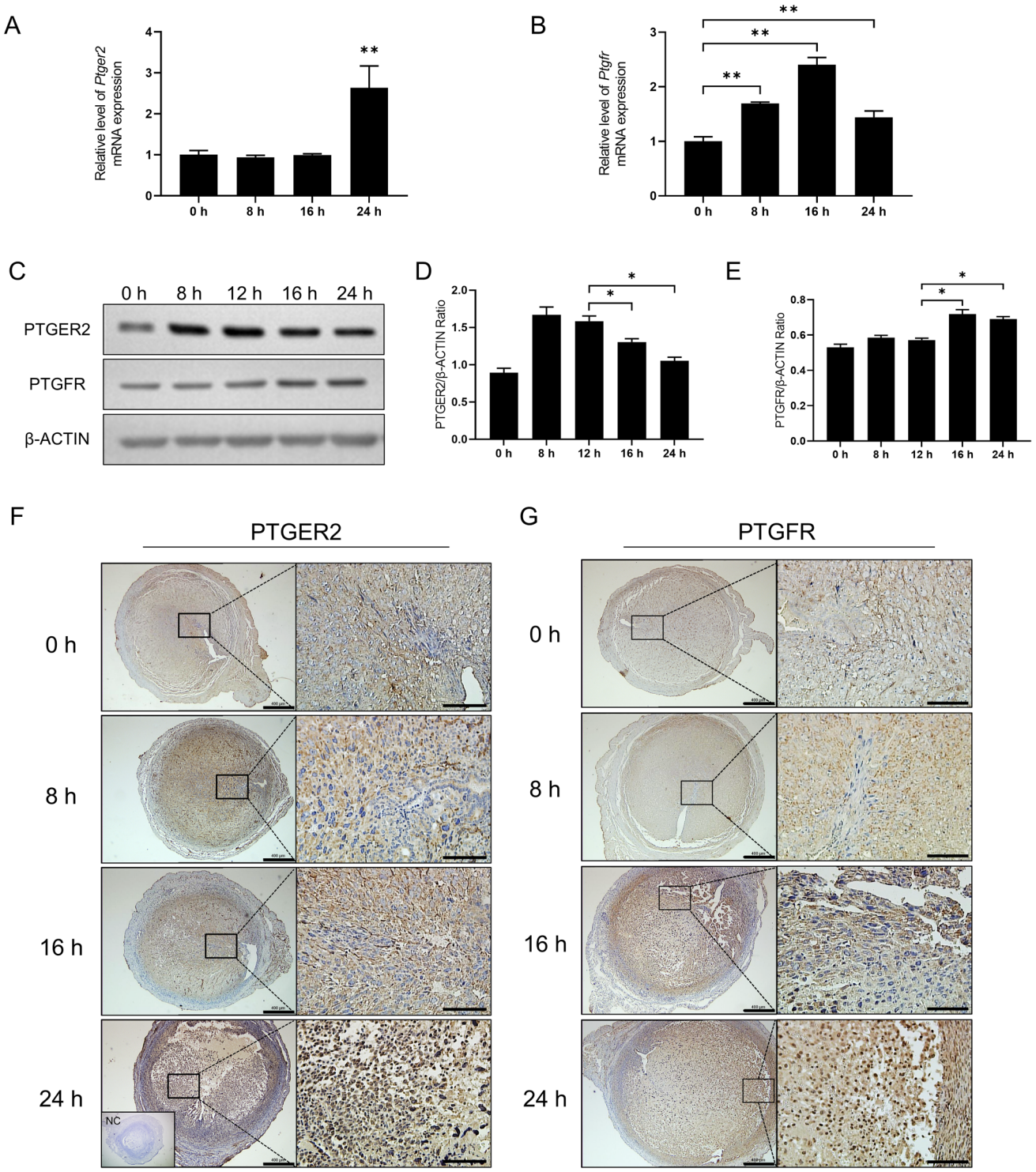

Fig. 2 The expressions of PTGER2 and PTGFR in the mice menstrual-like model at 0 h, 8 h, 16 h and 24 h after P4 withdrawal **A**: *Ptger2* mRNA expression levels investigated using real-time PCR. **B**: *Ptgfr* mRNA expression levels investigated using real-time PCR. **C-E**: Western blot analysis and gray value calculation of PTGER2 and PTGFR protein level in the mice menstrual-like model. (*$P<0.05$, **$P<0.01$, $n=3$) **F-G**: Immunohistochemistry staining of PTGER2 (F) and PTGFR (G) protein in the mice uterine. (The left panel scale bar = 400um; the right panel scale bar = 100 μm. NC = Negative control.)

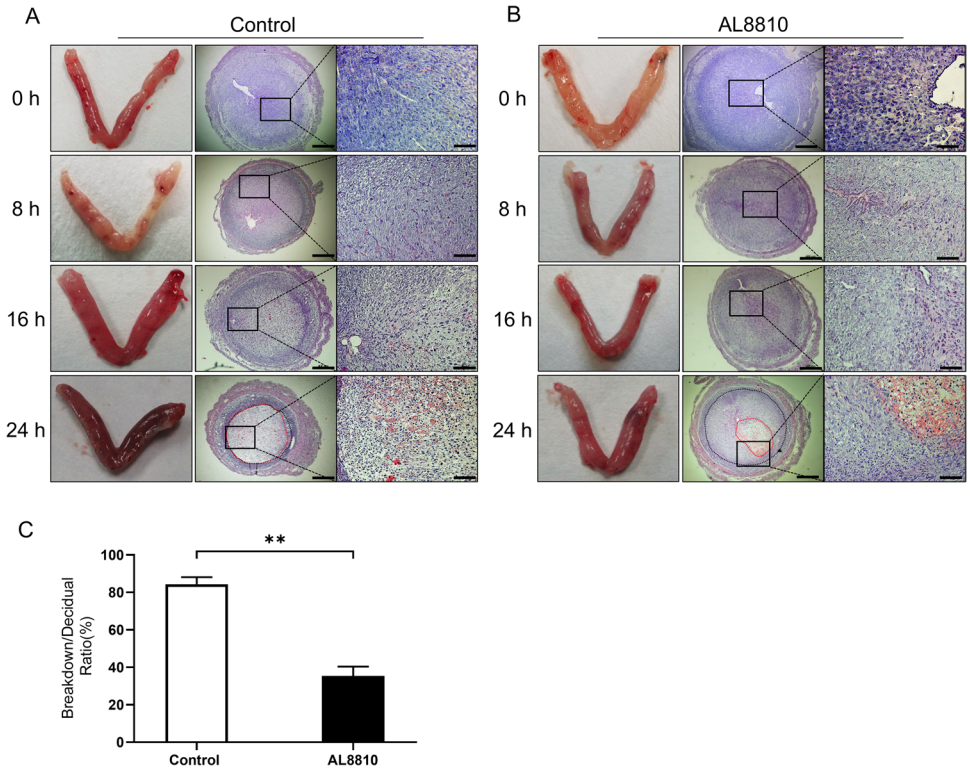

Fig. 3 The effect of PTGFR on the endometrial breakdown in the mice menstrual-like after P4 withdrawal **A-B**: The mouse uterine horns and the endometrial histology changes in control group (**A**) and PTGFR inhibitor (AL8810) treated group (**B**). (The left panel scale bar = 400um; the right panel scale bar = 100 μm.) **C**: The percentage of endometrial breakdown at 24 h after P4 withdrawal in control group and PTGFR inhibitor (AL8810) treated group. Black dash line circle = decidual zone; red dash line circle = breakdown zone. (**$P < 0.01$, $n = 3$)

concentrations results represent the vascular permeability in uterus. Evans blue concentration in uterus following the PTGFR inhibitor and HIF-1α inhibitor treatments were both significantly lower at 16 h after P4 withdrawal in comparison with that in the control group ($P = 0.0423$ and $P = 0.0343$ respectively) (Fig. 4E, F) [12]. These data confirmed that PTGFR inhibition suppressed vascular permeability and its relative factors Angiostatin and VEGF expression.

PTGFR Regulation by HIF-1α in Endometrial Breakdown

The regulatory relationship between PTGFR and HIF-1α was assessed. Firstly, immunohistochemical staining of serial sections revealed consistent localization of PTGFR and HIF-1α at 16 h and 24 h after P4 withdrawal in the mouse menstrual-like model (Fig. 5A). At 16 h after P4 withdrawal, PTGFR was localized in the cytoplasm, while HIF-1α was predominantly found in the nucleus. However, both PTGFR and HIF-1α were confined to the luminal epithelium and the pre-decidualized zone. At 24 h after P4 withdrawal, immunostaining of PTGFR and HIF-1α proteins in the pre-primary zone gave stronger results than at 16 h after P4 withdrawal; this is the main zone from where the endometrium shed. Furthermore, similarly to the PTGFR inhibitor, the HIF-1α inhibitor inhibited endometrial breakdown was revealed by HE staining (Fig. 5B).

To define the direct regulatory relationship of HIF-1α to *Ptgfr*, we applied ChIP assay that indicated the binding rate of HIF-1α to *Ptgfr* promoter. In mouse menstrual-like model, the percent of input of *Ptgfr* promoter binding with HIF-1α was relatively low at 0 h, while significantly increased at 16 h after P4 withdrawal (Fig. 5C).

The regulating mode where further investigated by *Ptgfr* mRNA and protein levels in the mouse menstrual-like model after HIF-1α inhibitor administration. At 8 h, there were no significance in *Ptgfr* mRNA between the inhibitor treatment group to the control group; however, at 16 h and 24 h, *Ptgfr* mRNA in the treatment groups was significantly lower than that in the control group ($P < 10^{-4}$ and $P = 0.0028$) (Fig. 5D). Meanwhile, PTGFR protein levels in the treatment group were also obviously lower than those in the control group at 16 h ($P = 0.0017$) (Fig. 5E). HIF-1α protein levels in the uterus were analyzed from 8 -24 h after P4 withdrawal (Fig. 5F). In the control group, HIF-1α protein levels in the nucleus increased by 16 h and then decreased at 24 h, relative to the levels at 8 h. HIF-1α inhibitor 2ME significantly lower the levels of HIF-1α at 16 h ($P < 10^{-4}$) in comparison to the control groups, which ensures the efficiency of HIF-1α inhibitor. HIF-1α inhibition significantly reduced the expressions of PTGFR in the mouse menstrual-like model.

PTGFR Regulation by HIF-1α in vitro in Human Stroma Cells Relevant to Menstruation

To further explore whether PTGFR is regulated by HIF-1α in human, we applied decidual-like human endometrial stromal

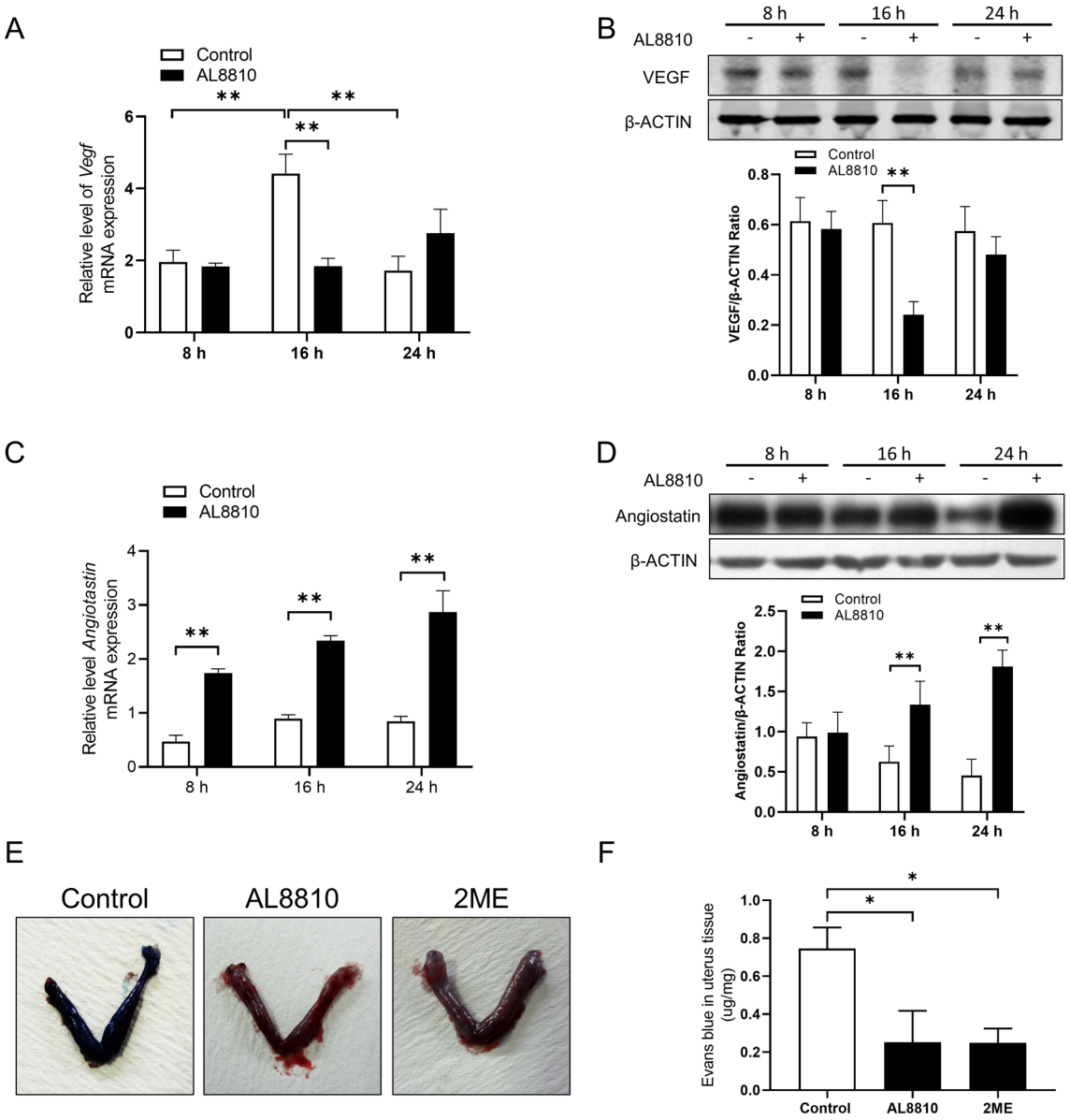

Fig. 4 The effect of PTGFR inhibitors on expressions of VEGF and Angiostatin, and vascular permeability in the mice menstrual-like after P4 withdrawal **A-B**: Real-time PCR results indicated the relative mRNA expressions of *Vegf* (**A**) and *Angiostatin* (**B**) in control group and PTGFR inhibitor (AL8810) treated group. **C-D**: Western blot analysis and gray value calculation of VEGF (**C**) and Angiostatin (**D**) protein level in the menstrual-like model. **E**: Macroscopic of mouse uterus at 16 h by Evans blue administration in the AL8810 and 2ME treatment groups to explored vascular permeability. **F**: Evans blue concentration in the AL8810 and 2ME treatment groups and the control group. (*$P<0.05$, **$P<0.01$, $n=3$)

cells following steroid deprivation, which mimicked the process of menstruation in vitro. Firstly, the decidual marker prolactin significantly increased from 4–8 days of decidual inducement ($P=0.0015$, $P=0.0028$ and $P=0.0068$ respectively) (Fig. 5G). It was also observed that the morphology of HESC after 8 days of decidual inducement showed characteristics of decidualization, that were larger nuclei and abundant cytoplasm. The deprivation of steroid in culture medium was marked as 0 h.

siRNA-*HIF-1α* knock down efficiency was verified by mRNA quantification. *HIF-1α* mRNA expression was significantly suppressed by siRNA-*HIF-1α* knock down compared with the siRNA-scrambled (negative) control group ($P<10^{-4}$) (Fig. 5H). The expression levels of *PTGFR* mRNA increased at 16 h after P4 withdrawal ($P=0.0054$). P4 withdrawal elevated *PTGFR* mRNA expression at 16 h ($P=0.0054$), while siRNA-*HIF-1α* treatment significantly inhibited *PTGFR* mRNA

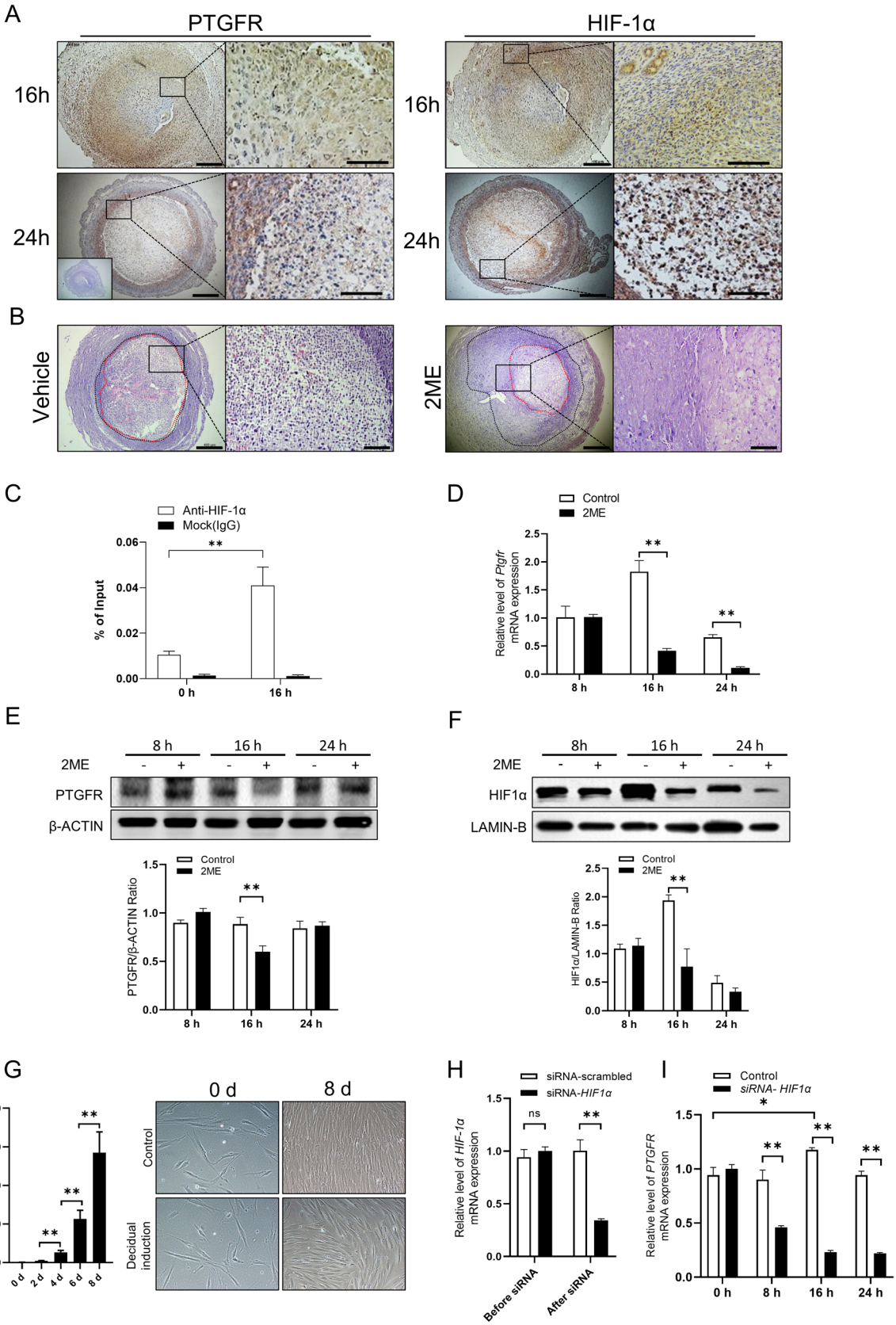
A
PTGFR
HIF-1α
16h
24h
16h
24h
B
Vehicle
2ME
C
Anti-HIF-1α
Mock(IgG)
% of Input
0.06
0.04
0.02
0.00
**
0 h
16 h
D
Control
2ME
Relative level of Ptgfr mRNA expression
2.5
2.0
1.5
1.0
0.5
0.0
**
**
8 h
16 h
24 h
E
8 h
16 h
24 h
2ME
- + - + - +
PTGFR
β-ACTIN
Control
2ME
PTGFR/β-ACTIN Ratio
1.5
1.0
0.5
0.0
**
8 h
16 h
24 h
F
8h
16 h
24 h
2ME
- + - + - +
HIF1α
LAMIN-B
Control
2ME
HIF1α/LAMIN-B Ratio
2.5
2.0
1.5
1.0
0.5
0.0
**
8 h
16 h
24 h
G
PRL concentration in HESC supernatant (ng/μl)
40
30
20
10
0
**
**
**
0 d
2 d
4 d
6 d
8 d
0 d
8 d
Control
Decidual induction
H
siRNA-scrambled
siRNA-HIF1α
Relative level of HIF-1α mRNA expression
1.5
1.0
0.5
0.0
ns
**
Before siRNA
After siRNA
I
Control
siRNA- HIF1α
Relative level of PTGFR mRNA expression
1.5
1.0
0.5
0.0
*
**
**
**
0 h
8 h
16 h
24 h

◂**Fig. 5** The PTGFR was regulated by HIF-1α during endometrial breakdown. **A**: Immunohistochemistry of PTGFR and HIF-1α protein in the mouse uterine at 16 h and 24 h after P4 withdrawal. (The left panel scale bar = 400um; the right panel scale bar = 100μm. NC = Negative control;) **B**: The uterine histomorphology of the mouse menstrual-like model at 24 h in control group and HIF-1α inhibitor (2ME) treated group. Black dash line = decidual zone; red dash line = breakdown zone. (The left panel scale bar = 400um; the right panel scale bar = 100μm.) **C**: The ChIP assay with the HIF-1α antibody to uterus at 0 h and 16 h. Real-time PCR were performed with the primers of Ptgf promoter region, and values were corrected for Input DNA as a ratio (white column). The negative control (Mock IgG) represents the IP background (dark column). **D**: Real-time PCR results indicated the relative mRNA expressions of Ptgfr in mouse menstrual-like model in control group and HIF-1α inhibitor (2ME) treated group. E-F: Western blot analysis and gray value calculation of PTGFR (**E**) and HIF-1α (**F**) protein in control group and 2ME treated group. **G**: T-HESC decidualization inducements. The chemiluminescence was used to detect PRL concentration in cell culture supernatant. Cell morphology of non-induced and induced decidualized cells (X200) was also observed. **H-I**: Real-time PCR results of and HIF-1α (**H**) before and after siRNA knock down, and PTGFR (**I**) in decidual T-HESC with or without siRNA-HIF-1α treatment at 0-24 h after P4 withdrawal. (*$P < 0.05$, **$P < 0.01$, $n = 3$)

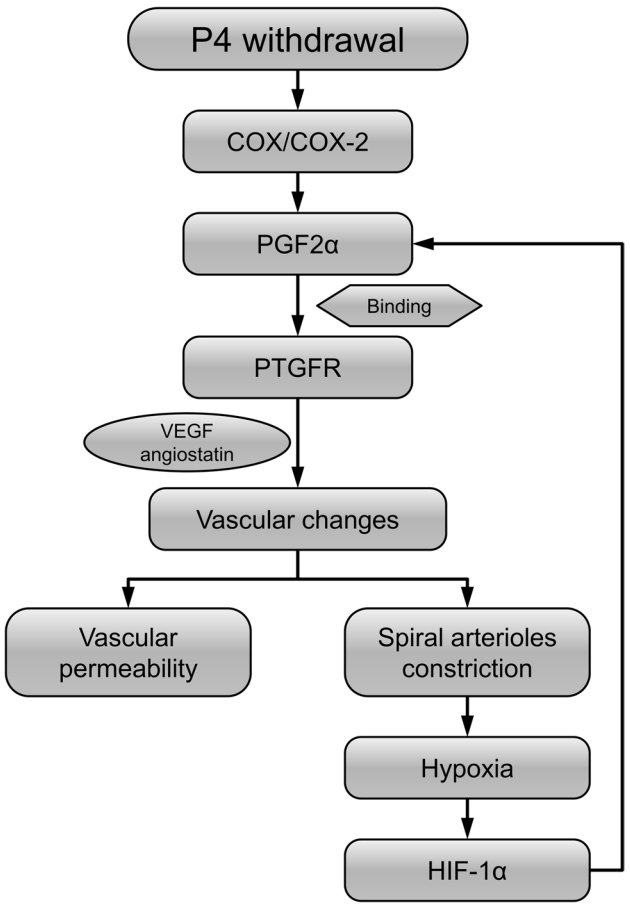

Fig. 6 The summary of PGF2α and PTGFR related signaling pathways in menstruation

expression from 8 to 24 h after P4 withdrawal compared to that in the control group (all $P < 10^{-4}$) (Fig. 5I).

Discussion

In this study, we first explored different types of PGs, and their receptors in the mice uterus during endometrial breakdown which suggested that PTGF2α and PTGFR was strongly involved. This was further confirmed by PTGFR inhibitor administration that significantly suppressed endometrial breakdown. Molecular regulation mechanism investigation revealed that PTGFR inhibition suppressed angiostatin expressions and vascular permeability and HIF-1α was also involved by directly binding to PTGF gene promoter. At last, PTGFR regulated by HIF-1α in vitro was investigated in human stroma cells relevant to menstruation.

Investigation of PGs levels in mouse uterus showed, except for PGI2, all PGs levels including PGE1, PGE2, and PGF2α increased during endometrial breakdown and shedding. In previous studies, PGE2 and PGF2α were found in the menstrual fluid of women [1], and especially elevated in the secretory phase and during menstruation [20]. The changes of PGE and PGF2α in our study are consistent with previously reported data, which indicated that they play a key role during endometrial breakdown and shedding. Interestingly, PGE2 and PGF2α function through their PTGER2 and PTGFR receptors, respectively [21]. Therefore, PTGER2 and PTGFR expression during endometrial breakdown was explored. The mRNA levels of *Ptger2* did not increase until 24 h after P4 withdrawal, while the protein level gradually decreased from 8–24 h; *Ptgfr* mRNA increased soon after P4 withdrawal at 8 h, increased steadily at 16 h, and decreased while endometrium breakdown completed at 24 h, that is PTGFR protein were highest during endometrial shedding, which indicated PTGFR has a closer relationship than PTGER2 with endometrial breakdown and shedding. However, there has been no comparison of P4 receptor proteins in humans with our data from mice; thus, further exploration is warranted. Further, a PTGFR inhibitor was administrated to the mice in our study, and the uterine and histological morphology showed that the decidualized stoma zone shedding was significantly inhibited in comparison to the control group, which provide a substantial evidence that PTGFR plays a critical role in endometrial breakdown and shedding. Although the hypothesis that increased production of PGF2α leads to myometrial contractions, vasoconstriction, and the onset of menstruation is generally accepted [22], the role of PTGFR in endometrial breakdown and shedding has been demonstrated for the first time.

Downstream regulation of PTGFR was also explored in the present study. As PGF2α/PTGFR may exert its effects via vascular changes, the related genes *VEGF*, and Angiostatin

were studied. Here, the PGF2α/PTGFR inhibitor markedly decreased *Vegf* mRNA and protein expression at 16 h, indicating that PGF2α/PTGFR positively regulated *VEGF* in the process, these results were consistent with previous study in bovine endometrial explants [23] and in the proliferation of endometrial endothelial cells [24, 25]. In addition, we found that the PGF2α/PTGFR inhibitor promoted Angiostatin mRNA and protein expression, so PGF2α/PTGFR negatively regulated Angiostatin in the process. VEGF plays a key role in promoting angiogenesis and increasing vascular permeability [10, 26]; however, Angiostatin has the opposite effect, that is inhibiting angiogenesis and reducing vascular permeability [10, 26]. Vascular permeability of the uterus was reduced by PGF2α/PTGFR inhibitor indicating associated with VEGF and Angiostatin during endometrial breakdown and shedding. Meanwhile, we also found that HIF-1α inhibitor suppressed vascular permeability in mouse menstrual-like model. In fact, HIF-1α play a role not only in endometrial breakdown but also in endometrial repair [12, 27]. In previous studies, it had been demonstrated that HIF-1α increase VEGF level during endometrial breakdown and repair [12, 28]. Whether or not HIF-1α regulates PTGFR during endometrial breakdown is another topic of interest. Interestingly, we found HIF-1α directly binds with *Ptgfr* promoter, and a HIF-1α inhibitor not only reduced PTGFR expression, but also blocked the breakdown and shedding, as well as the vascular permeability induced by PTGFR. Similar regulation patterns of HIF-1α and PTGFR were also found to occur in human stromal cells related to menstruation in vitro. Collectively, these results indicate that PTGFR is positively regulated by HIF-1α during endometrial breakdown. It might be the case that P4 withdrawal triggers an increase in cyclooxygenase (COX-2) levels and an increase in PGF2α synthesis, while high PGF2α/PTGFR levels regulate VEGF and Angiostatin to induce vascular changes, including vascular permeability and spiral arteriole constriction, causing hypoxia and inducing HIF-1α production, which in turn positively regulates PTGFR (Fig. 6). In our earlier research, we observed the histomorphological changes at various time points (0, 8, 16, 24 h) after P4 withdrawal in a mouse menstrual model. We noticed that localized necrosis of the subepithelial stromal cells in the endometrium began at 8 h, and by 24 h, the whole uterus endometrium was completely disintegrated [29]. Subsequently, P4 was replenished at 8, 12, 16, and 24 h after its withdrawal, and it was found that 16 h is a critical irreversible time point post-P4 withdrawal [30]. Therefore, the selection of time points in this study was based on the focus of the content to be demonstrated.

In summary, our study provides evidence that PGF2α/PTGFR plays a vital role in endometrial breakdown via effecting on vascular permeability, which regulated by HIF-1α. We investigated the dynamic changes in PGE1, PGE2, PGF2α, PGER2 and PTGFR levels during endometrial breakdown in a mouse menstrual-like model. PTGFR inhibitor blocked endometrial breakdown, reduced vascular permiability, down-regulated VEGF and upregulated Angiostatin. HIF-1α bound *Ptgfr* promoter and promoted PTGFR expression. Our findings are possibly useful for the clinic treatment of menstrual disorders and other related diseases.

Acknowledgements We would like to express our gratitude to Professor Haibin Wang, Laboratory of Xiamen University, for kindly offering the T-HESCs. The abstract graph was drawn by Figdraw.

Author's contribution X.X. study supervisor and fund acquisition; F.Z. and W.L. conceived and designed the experiments; F.Z. and S.G. operated the experiments; F.Z., X.C. and C.L. statistical analysis and data visualization; Z.L., X.Z., S.W. and J.W. mouse model assistant; B.H. and T.Z. result interpretation; S.W.[4] wrote the manuscript.

Funding This work was funded by the National Natural Science Foundation of China (No. 81571410) and the Non-profit Central Research Institute Fund of the National Research Institute for Family Planning (No. 2023GJZD01, 2023GJZ04).

Data Availability The data supporting the findings of this study are available from the corresponding author upon reasonable request.

Declarations

Conflict of interest The authors have no conflict of interest to declare.

References

1. Pickles VR. A plain-muscle stimulant in the menstruum. Nature. 1957;180(4596):1198–9.
2. Weems CW, Weems YS, Randel RD. Prostaglandins and reproduction in female farm animals. Vet J. 2006;171(2):206–28.
3. Sato K, Seto K. The effect of Dioscorea esculenta powder on prostaglandin E2 and cytochrome c oxidase subunit 2 levels, menstrual pain, and premenstrual syndrome in young women: A randomized double-blind controlled trial. Nutr Health. 2022;2601060221130889.
4. Hofmann BM, et al. Development of an Intrauterine Device Releasing Both Indomethacin and Levonorgestrel During the First Months of Use: Pharmacokinetic Characterization in Healthy Women. Clin Pharmacokinet. 2023;62(1):113–26.
5. Martin JN Jr, Bygdeman M, Eneroth P. The influence of locally administered prostaglandin E2 and F2alpha on uterine motility in the intact non-pregnant human uterus. Acta Obstet Gynecol Scand. 1978;57(2):141–7.
6. Xu X, et al. Cyclooxygenase-2 regulated by the nuclear factor-κB pathway plays an important role in endometrial breakdown in a female mouse menstrual-like model. Endocrinology. 2013;154(8):2900–11.
7. Efimova O, Volokhov A, Hales CA. Injection of prostaglandin F2α into the bronchial artery in sheep increases the pulmonary vascular permeability to protein. Pulm Pharmacol Ther. 2007;20(2):167–71.
8. Kaczynski P, Waclawik A. Effect of conceptus on expression of prostaglandin F2α receptor in the porcine endometrium. Theriogenology. 2013;79(5):784–90.

9. O'Reilly MS, et al. Angiostatin: a novel angiogenesis inhibitor that mediates the suppression of metastases by a Lewis lung carcinoma. Cell. 1994;79(2):315–28.
10. Cao Y, et al. Kringle domains of human angiostatin. Characterization of the anti-proliferative activity on endothelial cells. J Biol Chem. 1996;271(46):29461–7.
11. Baird DT, et al. Prostaglandins and menstruation. Eur J Obstet Gynecol Reprod Biol. 1996;70(1):15–7.
12. Chen X, et al. Vascular endothelial growth factor (VEGF) regulation by hypoxia inducible factor-1 alpha (HIF1A) starts and peaks during endometrial breakdown, not repair, in a mouse menstrual-like model. Hum Reprod. 2015;30(9):2160–70.
13. Chen X, et al. Hypoxia: involved but not essential for endometrial breakdown in mouse menstural-like model. Reproduction. 2020;159(2):133–44.
14. Wang GL, et al. Hypoxia-inducible factor 1 is a basic-helix-loop-helix-PAS heterodimer regulated by cellular O2 tension. Proc Natl Acad Sci U S A. 1995;92(12):5510–4.
15. Maybin JA, et al. The regulation of vascular endothelial growth factor by hypoxia and prostaglandin F(2)alpha during human endometrial repair. J Clin Endocrinol Metab. 2011;96(8):2475–83.
16. Brasted M, et al. Mimicking the events of menstruation in the murine uterus. Biol Reprod. 2003;69(4):1273–80.
17. Wang S, et al. CXCR4, regulated by HIF1A, promotes endometrial breakdown via CD45(+) leukocyte recruitment in a mouse model of menstruation. Reprod Biol. 2023;23(3): 100785.
18. Li Y, et al. The nuclear factor-κB pathway is involved in matrix metalloproteinase-9 expression in RU486-induced endometrium breakdown in mice. Hum Reprod. 2012;27(7):2096–106.
19. Yuhki M, et al. Establishment of an immortalized human endometrial stromal cell line with functional responses to ovarian stimuli. Reprod Biol Endocrinol. 2011;9:104.
20. Catalano RD, et al. Comprehensive expression analysis of prostanoid enzymes and receptors in the human endometrium across the menstrual cycle. Mol Hum Reprod. 2011;17(3):182–92.
21. Wang Q, et al. Prostaglandin Pathways: Opportunities for Cancer Prevention and Therapy. Can Res. 2022;82(6):949–65.
22. Ylikorkala O, Mäkilä UM. Prostacyclin and thromboxane in gynecology and obstetrics. Am J Obstet Gynecol. 1985;152(3):318–29.
23. Zhang S, et al. Prostaglandin F(2α)-PTGFR signalling activation, growth factor expression and cell proliferation in bovine endometrial explants. Reprod Fertil Dev. 2017;29(11):2195–205.
24. Jones MK, et al. Inhibition of angiogenesis by nonsteroidal anti-inflammatory drugs: insight into mechanisms and implications for cancer growth and ulcer healing. Nat Med. 1999;5(12):1418–23.
25. Sales KJ, et al. Expression, localization, and signaling of prostaglandin F2 alpha receptor in human endometrial adenocarcinoma: regulation of proliferation by activation of the epidermal growth factor receptor and mitogen-activated protein kinase signaling pathways. J Clin Endocrinol Metab. 2004;89(2):986–93.
26. Ji WR, et al. Characterization of kringle domains of angiostatin as antagonists of endothelial cell migration, an important process in angiogenesis. Faseb j. 1998;12(15):1731–8.
27. Maybin JA, et al. Hypoxia and hypoxia inducible factor-1α are required for normal endometrial repair during menstruation. Nat Commun. 2018;9(1):295.
28. Maybin JA, et al. Hypoxia and hypoxia inducible factor-1alpha are required for normal endometrial repair during menstruation. Nat Commun. 2018;9(1):295.
29. Xu X, He B, Wang J. Menstrual-like changes in mice are provoked through the pharmacologic withdrawal of progesterone using mifepristone following induction of decidualization. Hum Reprod. 2007;22(12):3184–91.
30. Wang Q, et al. A critical period of progesterone withdrawal precedes endometrial breakdown and shedding in mouse menstrual-like model. Hum Reprod. 2013;28(6):1670–8.